Title

Three-Dimensional Triple-Quantum Filtered Imaging of 0.012 M and 0.024 M Sodium-23 Using Fast Repetition Times

Authors

Keltner, J.R.
Wong, S.T.S.
Roos, M.S.

Publication Date

1992-07-01

LBL-32592
UC-000
Preprint

Lawrence Berkeley Laboratory
UNIVERSITY OF CALIFORNIA

Submitted to Journal of Magnetic Resonance

Three Dimensional Triple-Quantum Filtered Imaging of 0.012 M and 0.024 M Sodium-23 Using Fast Repetition Times

J.R. Keltner, S.T.S. Wong, and M.S. Roos

July 1992

Donner Laboratory

Biology & Medicine Division

Prepared for the U.S. Department of Energy under Contract Number DE-AC03-76SF00098

DISCLAIMER

LBL-32592
UC-000

Three Dimensional Triple-Quantum Filtered Imaging of 0.012 M and 0.024 M Sodium-23 Using Fast Repetition Times

J.R. Keltner, S.T.S. Wong, and M.S. Roos

Life Sciences Division
Lawrence Berkeley Laboratory
University of California
Berkeley, California 94720

July 1992

This work was supported by the National Heart, Lung, and Blood Institute under Grant HL 25840 and Grant HL 07367, by the National Science Foundation under Grant 89-02133, and by the U.S. Department of Energy under Contract No. DE-AC03-76SF00098.

Abstract

Efforts to improve the contrast in imaging sodium-23 (^{23}Na) with short relaxation times in biological tissues have lead to gradient-selected triple-quantum (GS3Q) filtered studies. The signal to noise ratio for GS3Q filtered experiments of ^{23}Na in agarose gels improves when the repetition time (T_R) decreases; however, spurious one-quantum (1Q) signals increase at short repetition times. We have developed a modification for the GS3Q filter to suppress these spurious 1Q signals. We calculate and experimentally verify that the GS3Q ^{23}Na signal to noise ratio for a fixed experimental time increases up to 100% as the T_R decreases from 300 ms to 55 ms for ^{23}Na in a 4% agarose gel. The suppression of spurious 1Q signals is improved by adding a preparatory crusher gradient and two-step phase cycling to the GS3Q filter. The T_R dependence of the suppression of spurious 1Q signals by the modified GS3Q filter are calculated and experimentally verified using an aqueous NaCl phantom. Using the modified GS3Q filter and a T_R of 70 ms, three dimensional triple-quantum filtered images of an 8.5 cm x 7 cm egg-shaped phantom containing 0.012 M NaCl and 0.024 M NaCl in a 4% agarose gel and 0.03 M NaCl in water were obtained with 1.5 x 1.5 x 1.5 cm^3 voxels (16 x 16 x 16 voxels). At 2.3 T the GS3Q filtered signal to noise ratios of the ^{23}Na in the agarose gel are 17 and 30 respectively for an imaging time of 54 minutes.

INTRODUCTION

In vivo multiple-quantum (MQ) filtered experiments are useful for selectively detecting ^{23}Na nuclei which are not in the fast motional narrowing limit and may prove useful for detecting ^{23}Na influx into the intracellular space (1,2,3). Gradient-selected MQ filters (4) have reduced dynamic range compared to phase cycled MQ filters because only the MQ signal is detected, and thus make less stringent demands upon electronics and digitizer resolution.

A significant difficulty of detecting *in vivo* MQ signals is their low signal to noise ratio (SNR). The SNR obtained in a fixed time may be increased by averaging signals from rapidly repeated experiments (5). Repetition times reported in the literature for ^{23}Na triple-quantum (3Q) filters typically range from 200 to 300 ms (1,2,6,7), although recently an experiment with a 105 ms repetition time was reported (8). We calculate and experimentally verify that the gradient-selected triple-quantum (GS3Q) ^{23}Na SNR increases up to 100% as the repetition time (T_R) decreases from 300 ms to 55 ms for ^{23}Na in a 4% agarose gel. Our measured relaxation times for ^{23}Na in a 4% agarose gel are similar to those from *in vivo* measurements (1).

This approach to increasing the GS3Q filtered *in vivo* ^{23}Na SNR is limited by how well the GS3Q filter suppresses unwanted single-quantum (1Q) ^{23}Na signals at short T_R. The suppression can be improved for short T_R by modifying the GS3Q filter with the addition of a preparatory crusher gradient and two step phase cycling. The preparatory crusher gradient helps to dephase transverse magnetization (9,10) so predominantly Z-magnetization remains for the subsequent 3Q filter. Two step phase cycling is employed to subtract 1Q signals

while adding 3Q signals (11).

Using the modified GS3Q filter and T_R of 70 ms, we have obtained GS3Q filtered images of a phantom containing 0.012 M and 0.024 M NaCl in 4% agarose gel spheres immersed in 0.03 M NaCl in water inside an egg-shaped container. The modified GS3Q filtered SNR of the ^{23}Na in the agarose gel are 17 and 30 respectively. The modified GS3Q filtered SNR of spurious 1Q signals from the ^{23}Na in the water is determined to be 1.5. The voxel size is 1.5 x 1.5 x 1.5 cm^3 and the imaging time is 54 minutes.

PULSE SEQUENCE

The modified GS3Q filter sequence incorporating a preparatory crusher gradient and two step phase cycling is displayed in figure 1. The first, third, fourth, fifth, seventh, and eighth RF pulses are 90° pulses. The second and sixth RF pulses are 180° pulses. The G_{3Q} gradient is in the x direction, while the crusher gradient is in the z direction. For imaging experiments, phase encoding pulses with the x, y, and z-gradients are used. The x-gradient phase encoding pulses are added to the G_{3Q} x-gradient waveform. Other parameters for the modified GS3Q filter are discussed in the Methods section.

THEORY

IRREDUCIBLE TENSOR OPERATOR REPRESENTATION OF DENSITY MATRIX

We calculate the signal from the modified gradient-selected 3Q filter using an irreducible tensor operator description of a spin 3/2 density matrix (12). There are sixteen elements of a spin 3/2 density matrix, but only ten are needed to describe quadrupole relaxation of ^{23}Na (13). It is convenient to represent the ten necessary elements of the density matrix as a column vector,

$$\rho = [\rho_{11}, \rho_{10}, \rho_{1(-1)}, \rho_{33}, \rho_{32}, \rho_{31}, \rho_{30}, \rho_{3(-1)}, \rho_{3(-2)}, \rho_{3(-3)}]^T. \quad [1]$$

The subscripts in the above representation of the density matrix correspond to the indices of the irreducible tensor operators.

Using a rotation matrix $R(\beta, \phi)$ and relaxation matrix $U(t, \delta\omega)$ it is possible to formulate an equation describing the action of a radio frequency (RF) hard pulse followed by relaxation,

$$\rho(t) = U(t, \delta\omega)R(\beta, \phi)\rho(0) + G(t). \quad [2]$$

Müller *et al.* have catalogued the elements of the rotation matrix $R(\beta, \phi)$ which describes the action of RF hard pulses (12). The RF flip angle and phase are represented by β and ϕ respectively.

$$R(\beta, \phi) = \begin{bmatrix} \begin{pmatrix} A_{ij}(\beta, \phi) \end{pmatrix} & \begin{pmatrix} 0 \end{pmatrix} \\ \begin{pmatrix} 0 \end{pmatrix} & \begin{pmatrix} B_{ij}(\beta, \phi) \end{pmatrix} \end{bmatrix}$$

The matrix $(A_{ij}(\beta, \phi))$ is 3×3 and $(B_{ij}(\beta, \phi))$ is 7×7. The elements $A_{ij}(\beta, \phi)$ and $B_{ij}(\beta, \phi)$ are listed in Table 1.

Jaccard *et al.* have similarly collected the elements of an evolution matrix $U(t, \delta\omega)$

which describes the quadrupole relaxation of ^{23}Na (13):

$$U(t,\delta\omega)=\begin{pmatrix}
C_{11}(t,\delta\omega) & 0 & 0 & 0 & 0 & D_{11}(t,\delta\omega) & 0 & 0 & 0 & 0 \\
0 & C_{22}(t) & 0 & 0 & 0 & 0 & D_{22}(t) & 0 & 0 & 0 \\
0 & 0 & C_{33}(t,\delta\omega) & 0 & 0 & 0 & 0 & D_{33}(t,\delta\omega) & 0 & 0 \\
0 & 0 & 0 & F_{11}(t,\delta\omega) & 0 & 0 & 0 & 0 & 0 & 0 \\
0 & 0 & 0 & 0 & F_{22}(t,\delta\omega) & 0 & 0 & 0 & 0 & 0 \\
E_{11}(t,\delta\omega) & 0 & 0 & 0 & 0 & F_{33}(t,\delta\omega) & 0 & 0 & 0 & 0 \\
0 & E_{22}(t) & 0 & 0 & 0 & 0 & F_{44}(t) & 0 & 0 & 0 \\
0 & 0 & E_{33}(t,\delta\omega) & 0 & 0 & 0 & 0 & F_{55}(t,\delta\omega) & 0 & 0 \\
0 & 0 & 0 & 0 & 0 & 0 & 0 & 0 & F_{66}(t,\delta\omega) & 0 \\
0 & 0 & 0 & 0 & 0 & 0 & 0 & 0 & 0 & F_{77}(t,\delta\omega)
\end{pmatrix}$$

The elements of $U(t,\delta\omega)$ are listed in Table 2. The relaxation times T_{1s} and T_{1f} characterize the relaxation of the Z-magnetization. The relaxation times T_{2s} and T_{2f} characterize the relaxation of the transverse magnetization. The relaxation times T_{22} and T_{23} respectively characterize the relaxation of the 2Q and 3Q coherences. The resonance offset is $\delta\omega$. The asterisks in Table 1 and Table 2 denote complex conjugation.

The vector $G(t)$ describes the relaxation of the Z-magnetization towards the thermal equilibrium magnetization,

$$G(t) = [0, d(1 - C_{22}(t)), 0, 0, 0, 0, -dE_{22}(t), 0, 0, 0]^T, \qquad [3]$$

where the density matrix representation of ^{23}Na nuclei in thermal equilibrium is

$$\rho_{eq} = [0, d, 0, 0, 0, 0, 0, 0, 0, 0]^T. \qquad [4]$$

CALCULATION OF STEADY STATE FOR GRADIENT-SELECTED 3Q FILTER

The evolution of the density matrix ρ caused by the application of the modified GS3Q filter may be written

$$\begin{aligned}\rho^{GS3Q}(\tau_s,\delta\omega_1,\delta\omega_2,\omega_{off}) &= T_8(\tau_s,\delta\omega_1,\delta\omega_2)[T_7(\delta\omega_1)[T_6[T_5[T_4(\tau_s,\delta\omega_1,\delta\omega_2)[T_3(\delta\omega_1)[T_2 \\ &\quad \times [T_1\rho_{eq}+G(\frac{\tau_1}{2})]+G(\frac{\tau_1}{2})]+G(\tau_2)]+G(\tau_{rg}+\tau_s+\tau_{cg})] \\ &\quad +G(\frac{\tau_1}{2})]+G(\frac{\tau_1}{2})]+G(\tau_2)]+G(\tau_{rg}+\tau_s+\tau_{cg}),\end{aligned} \quad [5]$$

where the T operators for the modified GS3Q filter are

$$T_1 = U(\frac{\tau_1}{2},\omega_{off})R(\frac{\pi}{2},0), \quad [6]$$

$$T_2 = U(\frac{\tau_1}{2},\omega_{off})R(\pi,\frac{\pi}{2}), \quad [7]$$

$$T_3(\delta\omega_1) = U(\tau_2,\omega_{off}+\delta\omega_1)R(\frac{\pi}{2},\frac{\pi}{2}), \quad [8]$$

$$T_4(\tau_s,\delta\omega_1,\delta\omega_2) = U(\tau_{cg},\omega_{off}+\delta\omega_2)U(\tau_s,\omega_{off})U(\tau_{rg},\omega_{off}+\delta\omega_1)R(\frac{\pi}{2},\frac{\pi}{2}), \quad [9]$$

$$T_5 = U(\frac{\tau_1}{2},\omega_{off})R(\frac{\pi}{2},\pi), \quad [10]$$

$$T_6 = U(\frac{\tau_1}{2},\omega_{off})R(\pi,-\frac{\pi}{2}), \quad [11]$$

$$T_7(\delta\omega_1) = U(\tau_2,\omega_{off}+\delta\omega_1)R(\frac{\pi}{2},-\frac{\pi}{2}), \quad [12]$$

$$T_8(\tau_s,\delta\omega_1,\delta\omega_2) = U(\tau_{cg},\omega_{off}+\delta\omega_2)U(\tau_s,\omega_{off})U(\tau_{rg},\omega_{off}+\delta\omega_1)R(\frac{\pi}{2},\frac{\pi}{2}). \quad [13]$$

The $\delta\omega_1$ term is included to describe off-resonance precession due to the G_{3Q} gradient. The $\delta\omega_2$ term is included to describe off-resonance precession due to the crusher gradient. The ω_{off} term is included to describe off-resonance precession due to inhomogeneities in the static magnetic field.

At sufficiently short repetition times the spins will not re-establish thermal equilibrium between subsequent applications of the modified GS3Q filter. Under these circumstances steady state transverse magnetization is established. The steady state density matrix is found by assuming that the density matrix has the same value immediately before the first RF pulse for subsequent modified GS3Q filters and solving Eq. [5] for $\rho_{ss}^{GS3Q}(\tau_s, \delta\omega_1, \delta\omega_2, \omega_{off})$,

$$\begin{aligned}\rho_{ss}^{GS3Q}(\tau_s, \delta\omega_1, \delta\omega_2, \omega_{off}) &= [I - T_8(\tau_s, \delta\omega_1, \delta\omega_2)T_7(\delta\omega_1)T_6T_5T_4(\tau_s, \delta\omega_1, \delta\omega_2)T_3(\delta\omega_1)T_2T_1]^{-1} \\ &\times (T_8(\tau_s, \delta\omega_1, \delta\omega_2)[T_7(\delta\omega_1)[T_6[T_5[T_4(\tau_s, \delta\omega_1, \delta\omega_2)[T_3(\delta\omega_1) \\ &\times [T_2G(\frac{\tau_1}{2}) + G(\frac{\tau_1}{2})] + G(\tau_2)] + G(\tau_{rg} + \tau_s + \tau_{cg})] \\ &+ G(\frac{\tau_1}{2})] + G(\frac{\tau_1}{2})] + G(\tau_2)] + G(\tau_{rg} + \tau_s + \tau_{cg})) .\end{aligned}$$

[14]

CALCULATION OF 3Q SIGNAL TO NOISE RATIO

The density matrix following the first G_{3Q} refocusing gradient is

$$\begin{aligned}\rho^{GS3Qa}(\tau_s, \delta\omega_1, \delta\omega_2, \omega_{off}) &= T_4^a(\delta\omega_1)[T_3(\delta\omega_1)[T_2[T_1\rho_{ss}^{GS3Q}(\tau_s, \delta\omega_1, \delta\omega_2, \omega_{off}) \\ &+ G(\frac{\tau_1}{2})] + G(\frac{\tau_1}{2})] + G(\tau_2)] + G(\tau_{rg}),\end{aligned}$$

[15]

where $T_4^a(\delta\omega_1) = U(\tau_{rg}, \omega_{off} + \delta\omega_1)R(\frac{\pi}{2}, \frac{\pi}{2})$. The density matrix following the second 3Q refocusing gradient is

$$\begin{aligned}\rho^{GS3Qb}(\tau_s, \delta\omega_1, \delta\omega_2, \omega_{off}) &= T_8^b(\delta\omega_1)[T_7(\delta\omega_1)[T_6[T_5[T_4^b(\tau_s, \delta\omega_2)\rho^{GS3Qa}(\tau_s, \delta\omega_1, \delta\omega_2, \omega_{off}) \\ &+ G(\tau_s + \tau_{cg})] + G(\frac{\tau_1}{2})] + G(\frac{\tau_1}{2})] + G(\tau_2)] + G(\tau_{rg}),\end{aligned}$$

[16]

where $T_8^b(\delta\omega_1) = U(\tau_{rg}, \omega_{off} + \delta\omega_1)R(\frac{\pi}{2}, \frac{\pi}{2})$ and $T_4^b(\tau_s, \delta\omega_2) = U(\tau_{rg}, \omega_{off} + \delta\omega_2)U(\tau_s, \omega_{off})$. Taking the difference of $\rho^{GS3Qa}(\tau_s, \delta\omega_1, \delta\omega_2, \omega_{off})$ and $\rho^{GS3Qb}(\tau_s, \delta\omega_1, \delta\omega_2, \omega_{off})$ and summing over spins with resonance offsets $\delta\omega_1$ and $\delta\omega_2$ each ranging from 0 to 2π yields

$$\Delta\rho^{GS3Q}(\tau_s, \omega_{off}) = \sum_{\delta\omega_1}\sum_{\delta\omega_2}\left(\rho^{GS3Qa}(\tau_s, \delta\omega_1, \delta\omega_2, \omega_{off}) - \rho^{GS3Qb}(\tau_s, \delta\omega_1, \delta\omega_2, \omega_{off})\right). \quad [17]$$

Using the (31) and (3(-1)) elements of $\Delta\rho^{GS3Q}(\tau_s, \omega_{off})$, the 3Q signal from the modified GS3Q filter is

$$S_{3Q}^{GS3Q}(t, \tau_s, \omega_{off}) = D'_{11}(t, 0)\frac{\rho_{3Q}^{GS3Q}(\tau_s, \omega_{off})}{D'_{11}(\tau_{rg}, 0)}, \quad [18]$$

where $\rho_{3Q}^{GS3Q}(\tau_s, \omega_{off}) = \frac{1}{\sqrt{2}}|\Delta\rho_{31}^{GS3Q}(\tau_s, \omega_{off}) - \Delta\rho_{3(-1)}^{GS3Q}(\tau_s, \omega_{off})|$ and $D'_{11}(t, 0) = \frac{\sqrt{6}}{5}(e^{-t/T'_{2f}} - e^{-t/T'_{2s}})$ (13). The form of $\rho_{3Q}^{GS3Q}(\tau_s, \omega_{off}^{\cdot})$ reflects that only one component of the transverse magnetization was detected since our RF coil was not used in quadrature. The transverse relaxation times T'_{2s} and T'_{2f} include the effects of inhomogeneities in the static field. The time origins for $D'_{11}(t, 0)$ immediately follow the fourth and eighth RF pulses. The signal is sampled from τ_{rg} to $\tau_{rg} + \tau_s$. $D'_{11}(t, 0)$ is evaluated on resonance in this calculation since we are only concerned with the magnitude of the modified GS3Q filtered signal.

The amplitude of the 3Q spectral line apodized with $D'_{11}(t, 0)$ is

$$A_{3Q}^{GS3Q} = \frac{\rho_{3Q}^{GS3Q}(\tau_s, \omega_{off})}{D'_{11}(\tau_{rg}, 0)}\int_{\tau_{rg}}^{(\tau_{rg}+\tau_s)}|D'_{11}(t, 0)|^2 dt. \quad [19]$$

The standard deviation of the apodized noise is

$$\sigma_a = \sigma\sqrt{\int_{\tau_{rg}}^{(\tau_{rg}+\tau_s)}|D'_{11}(t, 0)|^2 dt}, \quad [20]$$

where σ is the standard deviation of the noise. The ratio of A_{3Q}^{GS3Q} and σ_a give the apodized 3Q filtered signal to noise ratio obtained in a fixed time T_{exp},

$$\mathrm{SNR}_{3Q} = \sqrt{\frac{T_{exp}}{T_R}}\frac{\rho_{3Q}^{GS3Q}(\tau_s, \omega_{off})}{\sigma D'_{11}(\tau_{rg}, 0)}\sqrt{\int_{\tau_{rg}}^{(\tau_{rg}+\tau_s)}|D'_{11}(t, 0)|^2 dt}. \quad [21]$$

The term $\sqrt{T_{exp}/T_R}$ increases the SNR_{3Q} due to the averaging of a number of shots (5).

CALCULATION OF SUPPRESSION FACTOR

The suppression of 1Q signals is calculated by dividing the spurious 1Q signal from a modified GS3Q filtered experiment by the 1Q signal from a one pulse experiment. We designed the one pulse experiment by setting the amplitude of the G_{3Q} gradient to zero and by setting the flip angle of the first, second, third, fifth, sixth, and seventh pulses to zero. The steady state density matrix $\rho_{ss}^{OP}(\tau_s, \omega_{off})$ is obtained using Eq.[14] where in place of the T operators one uses

$$V_1 = U(\frac{\tau_1}{2}, \omega_{off})R(0,0), \quad [22]$$

$$V_2 = U(\frac{\tau_1}{2}, \omega_{off})R(0,0), \quad [23]$$

$$V_3 = U(\tau_2, \omega_{off})R(0,0), \quad [24]$$

$$V_4(\tau_s, \delta\omega_2) = U(\tau_{cg}, \omega_{off} + \delta\omega_2)U(\tau_s, \omega_{off})U(\tau_{rg}, \omega_{off})R(\frac{\pi}{2}, \frac{\pi}{2}), \quad [25]$$

$$V_5 = U(\frac{\tau_1}{2}, \omega_{off})R(0,0), \quad [26]$$

$$V_6 = U(\frac{\tau_1}{2}, \omega_{off})R(0,0), \quad [27]$$

$$V_7 = U(\tau_2, \omega_{off})R(0,0), \quad [28]$$

$$V_8(\tau_s, \delta\omega_2) = U(\tau_{cg}, \omega_{off} + \delta\omega_2)U(\tau_s, \omega_{off})U(\tau_{rg}, \omega_{off})R(\frac{\pi}{2}, -\frac{\pi}{2}), \quad [29]$$

The density matrix $\Delta\rho^{OP}(\tau_s, \omega_{off})$ is calculated identically to $\Delta\rho^{GS3Q}(\tau_s, \omega_{off})$, except that the V operators are used in place of the T operators. Using the (11) and (1(-1)) elements of $\Delta\rho^{OP}(\tau_s, \omega_{off})$ the 1Q signal from the one pulse experiment is

$$S_{1Q}^{OP}(t, \tau_s, \omega_{off}) = C'_{11}(t,0)\frac{\rho_{1Q}^{OP}(\tau_s, \omega_{off})}{C'_{11}(\tau_{rg}, 0)}, \quad [30]$$

where $\rho_{1Q}^{OP}(\tau_s,\omega_{off}) = \frac{1}{\sqrt{2}}|\Delta\rho_{11}^{OP}(\tau_s,\omega_{off}) - \Delta\rho_{1(-1)}^{OP}(\tau_s,\omega_{off})|$ and $C'_{11}(t,0) = \frac{3}{5}e^{-t/T'_{2f}} + \frac{2}{5}e^{-t/T'_{2s}}$. The amplitude of an apodized 1Q spectral line from the one pulse experiment is

$$A_{1Q}^{OP} = \frac{\rho_{1Q}^{OP}(\tau_s,\omega_{off})}{C'_{11}(\tau_{rg},0)} \int_{\tau_{rg}}^{(\tau_{rg}+\tau_s)} C'_{11}(t,0)D'_{11}(t,0)dt, \qquad [31]$$

where the apodizing function $D'_{11}(t,0)$ is used.

The spurious contribution of 1Q coherences to the modified GS3Q filtered signal is determined by calculating $\Delta\rho^{GS3Q}(\tau_s,\omega_{off})$ with the operators $T_4^{1Q}(\tau_s,\delta\omega_1,\delta\omega_2,\omega_{off})$ and $T_8^{1Q}(\tau_s,\delta\omega_1,\delta\omega_2,\omega_{off})$ instead of with $T_4^a(\tau_s,\delta\omega_1,\delta\omega_2,\omega_{off})$ and $T_8^b(\tau_s,\delta\omega_1,\delta\omega_2,\omega_{off})$. The operators $T_4^{1Q}(\tau_s,\delta\omega_1,\delta\omega_2,\omega_{off})$ and $T_8^{1Q}(\tau_s,\delta\omega_1,\delta\omega_2,\omega_{off})$ use rotation matrices $R(\frac{\pi}{2},\frac{\pi}{2})$ and $R(\frac{\pi}{2},-\frac{\pi}{2})$ in which the elements B_{31}, B_{37},B_{51}, and B_{57} are replaced by zero. Using the (11) and (1(-1)) elements of this $\Delta\rho^{GS3Q}(\tau_s,\omega_{off})$, the spurious 1Q signal from the modified GS3Q filtered experiment is

$$S_{1Q}^{GS3Q}(t,\tau_s,\omega_{off}) = C'_{11}(t,0)\frac{\rho_{1Q}^{GS3Q}(\tau_s,\omega_{off})}{C'_{11}(\tau_{rg},0)} \qquad [32]$$

where $\rho_{1Q}^{GS3Q}(\tau_s,\omega_{off}) = \frac{1}{\sqrt{2}}|\Delta\rho_{11}^{GS3Q}(\tau_s,\omega_{off}) - \Delta\rho_{1(-1)}^{GS3Q}(\tau_s,\omega_{off})|$. The amplitude of an apodized 1Q spectral line from the modified GS3Q filtered experiment is

$$A_{1Q}^{GS3Q} = \frac{\rho_{1Q}^{GS3Q}(\tau_s,\omega_{off})}{C'_{11}(\tau_{rg},0)} \int_{\tau_{rg}}^{(\tau_{rg}+\tau_s)} C'_{11}(t,0)D'_{11}(t,0)dt, \qquad [33]$$

where the apodizing function $D'_{11}(t,0)$ is again used. The suppression factor is defined to be,

$$\text{Suppression Factor} = \frac{A_{1Q}^{GS3Q}}{A_{1Q}^{OP}}. \qquad [34]$$

CALCULATION OF SPURIOUS 1Q RATIO

The ratio of spurious 1Q signal from a modified GS3Q filtered experiment divided by the 3Q signal from a modified GS3Q filtered experiment is referred to as the spurious 1Q ratio,

$$\text{Spurious 1Q Ratio} = \frac{A_{1Q}^{GS3Q}}{A_{3Q}^{GS3Q}}. \qquad [35]$$

METHODS

METHODS FOR CHARACTERIZING MODIFIED GS3Q FILTER

The performance of the modified GS3Q filter is evaluated by calculating and experimentally verifying the dependence of SNR_{3Q}, the suppression factor, and the spurious 1Q ratio upon repetition time and upon resonance offset. Sodium in an agarose gel yields a 3Q signal (14). The modified GS3Q filtered ^{23}Na signals from a 4 cm diameter sphere containing 2.0 M NaCl in a 4% agarose gel were measured for different T_R and resonance offset. The noise was measured for different T_R by shifting the frequency of the RF by 20 kHz. The quality factor of our RF coil was 200, so the 20 kHz shift in the RF frequency reduced the efficiency of the RF coil by 5%. These experimental data were apodized with the function $D'_{11}(t,0)$. The relaxation parameters of the ^{23}Na in the 2.0 M NaCl and 4% agarose gel were measured using techniques described by Pekar and Leigh (15) and Rooney and Springer (16). Using the measured ^{23}Na relaxation rates of the 2.0 M NaCl in the 4% agarose gel, the SNR_{3Q}

from the Theory section was calculated for various T_R and resonance offsets and compared with the measured modified GS3Q filtered SNR.

Sodium in an aqueous NaCl solution does not give a 3Q signal, since the ^{23}Na ions are in the fast motional narrowing limit(13). Therefore any ^{23}Na signal detected from an aqueous NaCl solution using a 3Q filter is spurious 1Q signal. The suppression factor was determined by dividing the spurious 1Q signal obtained from a modified GS3Q filtered experiment using a 4 cm diameter sphere containing 2.0 M aqueous NaCl by the 1Q signal obtained from a one pulse experiment using the same phantom. The suppression factor was measured for various T_R. These experimental data were apodized with the function $D'_{11}(t,0)$. Using the measured ^{23}Na relaxation parameters of the 2.0 M aqueous NaCl phantom the suppression factor from the Theory section was calculated for various T_R and compared to the measured suppression factors.

The spurious 1Q ratio defined in the Theory section was also calculated and compared to measurements. Two calculations were performed using the spurious 1Q ratio. In the first, A_{1Q}^{GS3Q} was calculated using the measured relaxation parameters of 2.0 M aqueous NaCl. In the second, A_{1Q}^{GS3Q} was calculated using the measured relaxation parameters of 2.0 M NaCl in the 4% agarose gel. In both calculations A_{3Q}^{GS3Q} was obtained using the measured relaxation parameters of 2.0 M NaCl in the 4% agarose gel. The ratio of the measured modified GS3Q filtered spurious 1Q signal from 2.0 M aqueous NaCl and the measured modified GS3Q filtered signal from the 2.0 M NaCl in the 4% agarose gel were compared to the first ratio calculated above for various T_R and resonance offsets. These experimental data were apodized with the function $D'_{11}(t,0)$.

The modified GS3Q filter parameters for the above experiments are listed in Table 3. A 13 cm diameter and 16 cm long birdcage RF coil and a 40 cm bore 2.35 Tesla Bruker magnet were used. The RF coil was not driven in quadrature. The gradient amplitudes were chosen to yield adequate dephasing across the sample without inducing excessive eddy currents. Thirteen different repetition times were used for the experiments. The repetition times were changed with τ_s by taking different numbers of sample points. The sampling interval was 100 μs, thus T_R = 18.75 ms + 100 μs $\times$ (number sample points). The number of sample points ranged from 128 to 2800 points yielding repetition times of 32 to 300 ms. Frequency offsets were obtained by shifting the frequency of the RF pulses. The total time of each experiment was T_{exp} = 7 sec. To insure that the spins were in steady state, the modified GS3Q filter was run for a 7 sec preparation period before the experiment during which no sampling occurred.

Calculations using the analysis presented in the Theory section were performed using Mathematica (Wolfram Research, Inc.) on a IBM RS6000 workstation. A homogeneous two-dimensional group of 625 (25 x 25) spins was used in the calculation. For all of the theoretical calculations a single factor was used to scale the calculated results to match the amount of ^{23}Na and the RF coil sensitivity in the experiments.

IMAGING METHODS

Three Dimensional triple-quantum filtered images were obtained using three phase encoding gradients after the fourth and eighth RF pulses in the modified GS3Q filter. A 8.5

cm x 7 cm plastic egg containing two 4 cm diameter plastic spheres was used (phantom 1). The NaCl concentrations of phantom 1 were chosen based on the concentrations and volume fractions of intracellular and extracellular ^{23}Na in the brain (17). Phantom 1 contained a 0.03 M aqueous NaCl solution inside the egg and outside of the spheres, 0.012 M NaCl in a 4% agarose gel inside one sphere, and 0.024 M NaCl in a 4% agarose gel inside the other sphere. The experimental parameters for the modified GS3Q filtered image are listed in Table 4. A one pulse image of phantom 1 was taken using the sequence described in the Theory section with parameters listed in the caption for Figure 7. For both of the above images the data were zero-filled to 64 x 64 x 64 points. Phantom 2 consisted of a 8.5 cm x 7 cm plastic egg containing only a 0.3 M aqueous NaCl solution. The suppression factor for the imaging experiments was determined by dividing the signal strength of a modified GS3Q filtered image of phantom 2 by the signal strength of a one pulse image of phantom 2 which used the GS3Q image parameters listed in Table 4. These experimental data were apodized with the function $D'_{11}(t,0)$.

The spurious 1Q ^{23}Na signal from the 0.03 M aqueous NaCl solution in the modified GS3Q image of phantom 1 was obscured by the measurement noise. The amplitude of this spurious 1Q ^{23}Na signal in this image was determined by two methods. In the first method the signal amplitude of a modified GS3Q filtered image of phantom 2, which consists of 0.3 M aqueous NaCl, was divided by 10. In the second method a one pulse image of phantom 1 was taken using the GS3Q image parameters listed in Table 4. The maximum signal of this image, which was produced by 1Q signals from the 0.03 M aqueous NaCl, was multiplied by the suppression factor measured using phantom 2. These experimental data were also apodized with the function $D'_{11}(t,0)$.

RESULTS

RESULTS FOR CHARACTERIZATION OF MODIFIED GS3Q FILTER

Figure 2 shows that SNR_{3Q} increases 100% as T_R decreases from 300 ms to 55 ms. Figure 3 shows that the suppression factor also increases for decreasing T_R. For T_R less than 70 ms the suppression factor increases more rapidly since saturation reduces the signal obtained from the one pulse experiment. For T_R larger than 120 ms the experimental suppression factor for the 4 cm diameter sphere was approximately 1/2500. Figure 4 shows that the spurious 1Q ratio for the 2.0 M aqueous NaCl phantom increases up to 12% as the T_R decreases to 32 ms. For T_R of 70 ms the modified GS3Q filtered spurious 1Q signal from the 2.0 M aqueous NaCl phantom is approximately 5% of the modified GS3Q filtered signal from the 2.0 M NaCl and 4% agarose phantom. Figure 4 also shows that the calculated spurious 1Q signal from the 2.0 M NaCl in a 4% agarose gel is less than 1% of the calculated and measured modified GS3Q filtered 3Q signal from the 2.0 M NaCl in a 4% agarose gel for T_R as low as 32ms. The results displayed in Figure 4 demonstrate that ^{23}Na with shorter relaxation times produces less GS3Q filtered spurious 1Q signal for short T_R.

Figure 5 shows SNR_{3Q} plotted versus frequency offset. Calculated predictions and experimental measurements are included in Figure 5 for the off-resonance dependence of SNR_{3Q} from the modified GS3Q filter without the 180° refocusing pulses. The calculations were made by setting the flip angle of the refocusing rotation matrix in operators T_2 and T_6 to zero. The off-resonant frequency at which the non-refocused SNR_{3Q} reaches a mini-

mum corresponds to the nuclear spins having precessed $\frac{(2n+1)\pi}{2}$ $(n = 0, 1, 2, ...)$ during the preparation period. As the preparation time is shortened, the off-resonant frequency of the first minimum grows larger. Recently an imaging sequence in which the phase encoding is performed during the preparation period was proposed (18). The above results show that for GS3Q filters with long preparation periods (>5 ms), significant loss of signal may occur due to off-resonant spins. In Figure 6 the spurious 1Q ratio is plotted versus frequency offset.

The measured relaxation parameters of ^{23}Na in the 2.0 M NaCl, 4% agarose phantom are displayed in Table 5. The measured relaxation parameters of the ^{23}Na in water were T_1=50.0 $\pm$ 2.0 ms, T_2=49.0 $\pm$ 2.0 ms, and T_2'=32.0 $\pm$ 1.0 ms. The primed relaxation times include the effects of static field inhomogeneity. The increase in measurement error of the unprimed versus the primed relaxation times is due to limits of accuracy in measuring the contribution of static magnetic field inhomogeneities to the relaxation times.

IMAGING RESULTS

A one pulse image of phantom 1 is shown in Figure 7. A modified GS3Q filtered image of phantom 1 is shown in Figure 8. The modified GS3Q filtered SNR of the 0.012 M and 0.024 M NaCl, 4% agarose gel balls are 17 and 30. The suppression factor measured with phantom 2 was 220 for the center 1.5 x 1.5 x 1.5 cm^3 voxel and 450 for all of the other 1.5 x 1.5 x 1.5 cm^3 voxels. The decreased suppression factor for the center voxel is attributed to inadequate dephasing of steady state transverse magnetization. Both of the methods discussed in the Imaging Methods section to determine the amplitude of the spurious 1Q signal from the 0.03 M aqueous NaCl in the modified GS3Q filtered image of phantom 1 determine

the SNR of the spurious 1Q signal to be 1.5.

DISCUSSION

The results presented characterizing the modified GS3Q filter show that given the appropriate ^{23}Na relaxation parameters, it is possible to calculate the repetition time which maximizes SNR_{3Q}, as well as calculate the suppression factor and spurious 1Q ratio for that repetition time. An issue not considered here, but which may provide a lower limit for the repetition time in *in vivo* imaging experiments, is RF power deposited in the patient.

We predict that there will be approximately a factor of four reduction in SNR_{3Q} for a modified GS3Q filtered image of a human head compared to the modified GS3Q filtered image of phantom 1 displayed in Figure 8. This prediction is based upon the comparison of SNR measurements from a 30 cm diameter, 30 cm long, 22 Mhz ^{1}H RF Alderman and Grant head coil loaded by a patient and SNR measurements from the 26 Mhz ^{23}Na RF birdcage coil loaded by phantom 1. These measurements were made by determining the RF magnetic field produced per unit current for each coil and invoking reciprocity (19) and by measuring the noise for each coil. This prediction assumes the ^{23}Na in the human head has relaxation times similar to the relaxation times displayed in Table 5. To maintain the SNR_{3Q} and acquisition time of Figure 8 for a modified GS3Q filtered image of a human head, the voxel size would need to increase from 1.5 x 1.5 x 1.5 cm^3 to 2.0 x 2.0 x 2.0 cm^3 and the RF head coil would need to be used in quadrature. We conclude that quadrature modified GS3Q filtered imaging of a human head using T_R of 70 ms with 2.0 x 2.0 x 2.0 cm^3 voxels should

yield a SNR_{3Q} of 10 for 0.012 M ^{23}Na with relaxation times similar to those in Table 5 in a 30 minute experiment at 2.3 T.

ACKNOWLEDGMENTS

The authors are indebted to Jim Pekar for many helpful discussions. We are grateful to Thomas Budinger for his guidance and support, and to Blaise Frederick for the use of the ^{23}Na birdcage RF coil. This work was supported by the Director, Office of Energy Research, of the U.S. Department of Energy under Contract No. DE-AC03-76SF00098, by the National Heart, Lung and Blood Institute under Grant HL 25840 and Grant HL 07367, and by the National Science Foundation under Grant 89-20133.

REFERENCES

1. R.C. Lyon, J. Pekar, C.T.W. Moonen, and A.C. McLaughlin, *Mag. Res. Med.* **18**, 80(1991).

2. J. Pekar, L. Ligeti, Z. Ruttner, T. Sinnwell, C.T.W. Moonen, and A.C. McLaughlin, *SMRM Abstracts* **10**, 149(1991).

3. J.L. Allis, A.M.L. Seymour, and G.K. Radda, *J. Mag. Res.* **93**, 71(1991)

4. A. Bax, P.G. DeJong, and J. Smidt, *Chem. Phys. Let.* **69**(3), 567(1980).

5. E.R. Ernst and W.A. Anderson, *Rev. Sci. Instrum.* **37**, 93(1966).

6. R.H. Griffey, B.V. Griffey, N.A. and Matwiyoff, *Mag. Res. Med.* **13**, 305(1990).

7. M.D. Cockman, L.W. Jelinski, J. Katz, D.D. Sorce, L.M. Boxt, and P.J. Cannon, *J. Mag. Res.* **90**, 9(1990)

8. S. Wimperis and B. Wood., *J. Mag. Res.* **95**, 428(1991)

9. R. Kaiser, E. Bartholdi, R.R. and Ernst, *J. Chem. Phys.* **60**, 2966 (1974).

10. C.T.W. Moonen and P.C.M. Van Zigal, *J. Mag. Res.* **88**, 28(1990).

11. A. Bax, R. Freeman, and S.P. Kempsell, *Chem. Phys. Let.* **69**(3), 567(1980).

12. N. Müller, G. Bodenhausen, and R.R. Ernst, *J. Mag. Res.* **75**, 297(1987).

13. G. Jaccard, W. Wimperis, and G. Bodenhausen, *J. Chem. Phys.* **85**, 6282(1986).

14. J. Andrasko, *J. Mag. Res.* **16**, 502(1974)

15. J. Pekar, and J.S. Leigh, *J. Mag. Res.* **69**, 582(1986)

16. W.D. Rooney, and C.S. Springer, *NMR Biomed.* 4(5) 209(1991).

17. S.K. Hilal, A.A. Maudsley, J.B. Ra, H.E. Simon, P. Roschmann, S. Wittekeok, Z.H. Cho, and S.K. Mun, *J. Comp. Asst. Tomog.* **9**, 1(1985).

18. S. Wimperis, P. Cole, and P. Styles, "Triple-Quantum Filtration NMR Imaging of 200 mM Sodium at 1.9 Tesla," *J. Mag. Res.* (In Press).

19. D.I. Hoult and R.E. Richards, *J. Mag. Res.* **24**, 71(1976)

FIGURE CAPTIONS

Figure 1 Schematic representation of the modified gradient-selected triple-quantum filter with preparatory crusher gradient and two step phase cycling.

Figure 2 Triple-quantum filtered signal to noise ratio vs. repetition time for the modified gradient-selected triple-quantum filter. The solid line is the theoretical prediction of SNR_{3Q} as defined in the Theory section and the solid circles are the experimental data points. The sample is a 4 cm diameter sphere containing 2.0 M NaCl + 4% agarose. See text for parameters.

Figure 3 Suppression factor vs. repetition time for modified gradient-selected triple-quantum filter. The solid line is the theoretical prediction of the suppression factor as defined in the Theory section and the solid circles are the experimental data points. The sample is a 4 cm diameter sphere containing 2.0 M aqueous NaCl. See text for parameters.

Figure 4 Spurious 1Q ratio vs. repetition time for modified gradient-selected triple-quantum filter. The solid line is the theoretical prediction for the ratio of modified GS3Q filtered spurious 1Q signal from 2.0 M aqueous NaCl and modified GS3Q filtered 3Q signal from 2.0 M NaCl + 4% agarose. The dashed line is the theoretical prediction for the ratio of modified GS3Q filtered spurious 1Q signal from 2.0 M NaCl + 4% agarose and modified GS3Q filtered 3Q signal from 2.0 M NaCl + 4% agarose. The solid circles are the experimental data points for the ratio of modified GS3Q filtered spurious 1Q signal from 2.0 M aqueous NaCl and modified GS3Q filtered signal from 2.0 M NaCl + 4% agarose. The samples are 4 cm diameter spheres. See text for parameters.

Figure 5 Triple-quantum filtered signal to noise ratio vs. resonance offset. The solid line is the theoretical prediction of SNR_{3Q} as defined in the Theory section for the modified GS3Q filter. The dashed line is the theoretical prediction for the modified GS3Q filter without the 180° refocusing pulses. The solid circles and open squares are the experimental points for the modified GS3Q filter with and without the 180° refocusing pulses. The sample is a 4 cm diameter sphere containing 2.0 M NaCl and 4% agarose. The repetition time is 70 ms. For this experiment 256 points were sampled at a rate of $1/(200\ \mu s)$. The 256 sampled points were zero-filled up to 2256 points. See text for other parameters.

Figure 6 Spurious 1Q Ratio versus resonance offset. The solid line is the theoretical prediction for the ratio of modified GS3Q filtered spurious 1Q signal from 2.0 M aqueous NaCl and modified GS3Q filtered 3Q signal from 2.0 M NaCl + 4% agarose. The solid circles are the experimental data points for the ratio of modified GS3Q filtered spurious 1Q from 2.0 M aqueous NaCl and modified GS3Q filtered signal from 2.0 M NaCl + 4% agarose. The samples are 4 cm diameter spheres. For this experiment 256 points were sampled at a rate of $1/(200\ \mu s)$. The 256 sampled points were zero-filled up to 2256 points. See text for other parameters.

Figure 7 A one pulse image of phantom 1. Phantom 1 consists of a 8.5 cm x 7 cm plastic egg containing two 4 cm diameter plastic spheres. In between the egg and the spheres is 0.03 M aqueous NaCl. Inside one sphere is 0.012 M NaCl in a 4% agarose gel. Inside the other sphere is 0.024 M NaCl in a 4% agarose gel. The field of view in each dimension is 24 cm. The number of phase encodes in each dimension is 32. The voxel size is 0.75 x 0.75 x 0.75 cm^3. The repetition

time was 100 ms. The imaging time was 110 minutes. The data for this three dimensional image was zero-filled to 64 x 64 x 64 points. The above picture is a 64 x 64 x 1 voxel slice from the three dimensional image.

Figure 8 A modified GS3Q filtered image of phantom 1. The image parameters are listed in Table 4. The modified GS3Q filtered SNR of the 0.012 M NaCl, 4% agarose ball is 17. The modified GS3Q filtered SNR of the 0.024 M NaCl, 4% agarose ball is 30. The modified GS3Q filtered spurious 1Q signal from the 0.03 M aqueous NaCl has SNR of 1.5. The data for this three dimensional image was zero-filled to 64 x 64 x 64 points. The field of view in each dimension is 24 cm. The above picture is a 64 x 64 x 1 voxel slice from the three dimensional image.

TABLE 1

Elements of Rotation Matrix $R_{ij}(\beta,\phi)$

Matrix Elements	Value
$A_{11}(\beta,\phi)$,$A_{33}(\beta,\phi)$	$\cos^2\frac{\beta}{2}$
$A_{22}(\beta,\phi)$	$\cos\beta$
$A^*_{21}(\beta,\phi)$,$A^*_{32}(\beta,\phi)$,$-A_{12}(\beta,\phi)$,$-A_{23}(\beta,\phi)$	$e^{i\phi}\frac{1}{\sqrt{2}}\sin\beta$
$A^*_{31}(\beta,\phi)$,$A_{13}(\beta,\phi)$	$e^{2i\phi}\sin^2\frac{\beta}{2}$
$B_{11}(\beta,\phi)$,$B_{77}(\beta,\phi)$	$\cos^6\frac{\beta}{2}$
$-B^*_{12}(\beta,\phi)$,$-B^*_{67}(\beta,\phi)$,$B_{21}(\beta,\phi)$,$B_{76}(\beta,\phi)$	$e^{i\phi}\sqrt{6}\cos^5\frac{\beta}{2}\sin\frac{\beta}{2}$
$B^*_{13}(\beta,\phi)$,$B^*_{57}(\beta,\phi)$,$B_{31}(\beta,\phi)$,$B_{75}(\beta,\phi)$	$e^{2i\phi}\frac{\sqrt{15}}{8}\sin^2\beta(1+\cos\beta)$
$-B^*_{14}(\beta,\phi)$,$-B^*_{47}(\beta,\phi)$,$B_{41}(\beta,\phi)$,$B_{74}(\beta,\phi)$	$e^{3i\phi}\frac{\sqrt{5}}{4}\sin^3\beta$
$B^*_{15}(\beta,\phi)$,$B^*_{37}(\beta,\phi)$,$B_{51}(\beta,\phi)$,$B_{73}(\beta,\phi)$	$e^{4i\phi}\frac{\sqrt{15}}{8}\sin^2\beta(1-\cos\beta)$
$-B^*_{16}(\beta,\phi)$,$-B^*_{27}(\beta,\phi)$,$B_{61}(\beta,\phi)$,$B_{72}(\beta,\phi)$	$e^{5i\phi}\sqrt{6}\sin^5\frac{\beta}{2}\cos\frac{\beta}{2}$
$B^*_{17}(\beta,\phi)$,$B_{71}(\beta,\phi)$	$e^{6i\phi}\sin^6\frac{\beta}{2}$
$B_{22}(\beta,\phi)$,$B_{66}(\beta,\phi)$	$\frac{1}{4}(1+\cos\beta)^2(3\cos\beta-2)$
$B^*_{23}(\beta,\phi)$,$B^*_{56}(\beta,\phi)$,$-B_{32}(\beta,\phi)$,$-B_{65}(\beta,\phi)$	$e^{i\phi}\frac{\sqrt{10}}{8}\sin\beta(1-3\cos\beta)(\cos\beta+1)$
$B^*_{24}(\beta,\phi)$,$B^*_{46}(\beta,\phi)$,$B_{42}(\beta,\phi)$,$B_{64}(\beta,\phi)$	$e^{2i\phi}\sqrt{\frac{15}{8}}\sin^2\beta\cos\beta$
$B^*_{25}(\beta,\phi)$,$B^*_{36}(\beta,\phi)$,$-B_{52}(\beta,\phi)$,$-B_{63}(\beta,\phi)$	$e^{3i\phi}\frac{\sqrt{10}}{8}\sin\beta(1+3\cos\beta)(\cos\beta-1)$
$B^*_{26}(\beta,\phi)$,$B_{62}(\beta,\phi)$,	$e^{4i\phi}\frac{1}{4}(1-\cos\beta)^2(3\cos\beta+2)$
$B_{33}(\beta,\phi)$,$B_{55}(\beta,\phi)$	$\frac{1}{8}(1+\cos\beta)(15\cos^2\beta-10\cos\beta-1)$
$-B^*_{34}(\beta,\phi)$,$-B^*_{45}(\beta,\phi)$,$B_{43}(\beta,\phi)$,$B_{54}(\beta,\phi)$	$e^{i\phi}\frac{\sqrt{3}}{4}\sin\beta(5\cos^2\beta-1)$
$B^*_{35}(\beta,\phi)$,$B_{53}(\beta,\phi)$	$e^{2i\phi}\frac{1}{8}(1-\cos\beta)(15\cos^2\beta+10\cos\beta-1)$
$B_{44}(\beta,\phi)$	$\frac{1}{2}\cos\beta(5\cos^2\beta-3)$

TABLE 2

Elements of Evolution Matrix $U_{ij}(t, \delta\omega)$

Matrix Elements	Value
$C^*_{11}(t,\delta\omega)$,$C_{33}(t,\delta\omega)$	$e^{i\delta\omega t}(\frac{3}{5}e^{-t/T_{2f}} + \frac{2}{5}e^{-t/T_{2s}})$
$C_{22}(t)$	$\frac{1}{5}e^{-t/T_{1f}} + \frac{4}{5}e^{-t/T_{1s}}$
$D_{11}(t,\delta\omega)$,$E_{11}(t,\delta\omega)$,$D^*_{33}(t,\delta\omega)$,$E^*_{33}(t,\delta\omega)$	$e^{i\delta\omega t}\frac{\sqrt{6}}{5}(e^{-t/T_{2f}} - e^{-t/T_{2s}})$
$D_{22}(t)$,$E_{22}(t)$	$\frac{2}{5}(e^{-t/T_{1f}} - e^{-t/T_{1s}})$
$F_{11}(t,\delta\omega)$,$F^*_{77}(t,\delta\omega)$	$e^{i3\delta\omega t}e^{-t/T_{23}}$
$F_{22}(t,\delta\omega)$,$F^*_{66}(t,\delta\omega)$	$e^{i2\delta\omega t}e^{-t/T_{22}}$
$F_{33}(t,\delta\omega)$,$F^*_{55}(t,\delta\omega)$	$e^{i\delta\omega t}(\frac{2}{5}e^{-t/T_{2f}} + \frac{3}{5}e^{-t/T_{2s}})$
$F_{44}(t)$	$\frac{4}{5}e^{-t/T_{1f}} + \frac{1}{5}e^{-t/T_{1s}}$

TABLE 3

Modified Gradient-Selected Triple-Quantum Filter Parameters

Parameter	Value
3Q Gradient Filter Amplitude	0.7 G/cm
Crusher Gradient Amplitude	0.3 G/cm
90° RF Pulse Duration	140 μs
180° RF Pulse Duration	280 μs
τ_1	$ln(T_{2f}/T_{2s})/((1/T_{2s}) - 1/T_{2f})$ (Ref 13)
τ_2	1 ms
τ_{rg}	3.0 ms
τ_{cg}	5.0 ms

TABLE 4

Three Dimensional Gradient-Selected Triple-Quantum Filtered Image Parameters

Parameter	Value
Modified GS3Q Filter Parameters	Same as in Table 3
Number of Phase Encodes in Each Dimension	16
Field of View in Each Dimension	24 cm
Voxel Size	1.5 x 1.5 x 1.5 cm^3
T_R	70 ms
Imaging Time	54 minutes

TABLE 5

Measured Relaxation Parameters of 2.0 M NaCl + 4% Agarose Phantom

Parameter	Value (ms)	Parameter	Value (ms)
T_{1s}	24.6 ± 2.0	T_{23}	24 ± 8
T_{1f}	16.6 ± 2.0	T'_{2s}	19 ± 1
T_{2s}	22 ± 3	T'_{2f}	3.5 ± 0.1
T_{2f}	3.6 ± 0.2	T'_{22}	3.4 ± 0.
T_{22}	3.6 ± 0.2	T'_{23}	17 ± 1

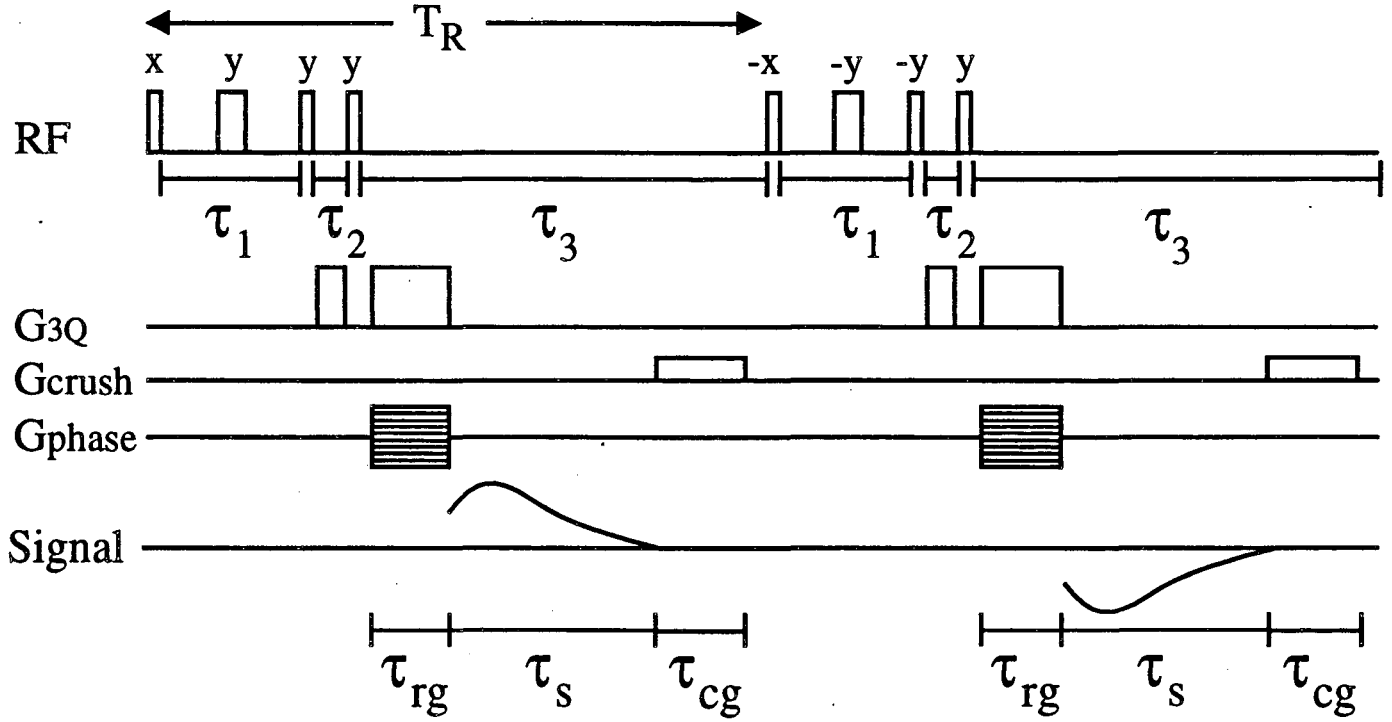
T_R
x y y y -x -y -y y
RF
τ_1 τ_2 τ_3 τ_1 τ_2 τ_3
G3Q
Gcrush
Gphase
Signal
τ_{rg} τ_s τ_{cg} τ_{rg} τ_s τ_{cg}

Figure 1

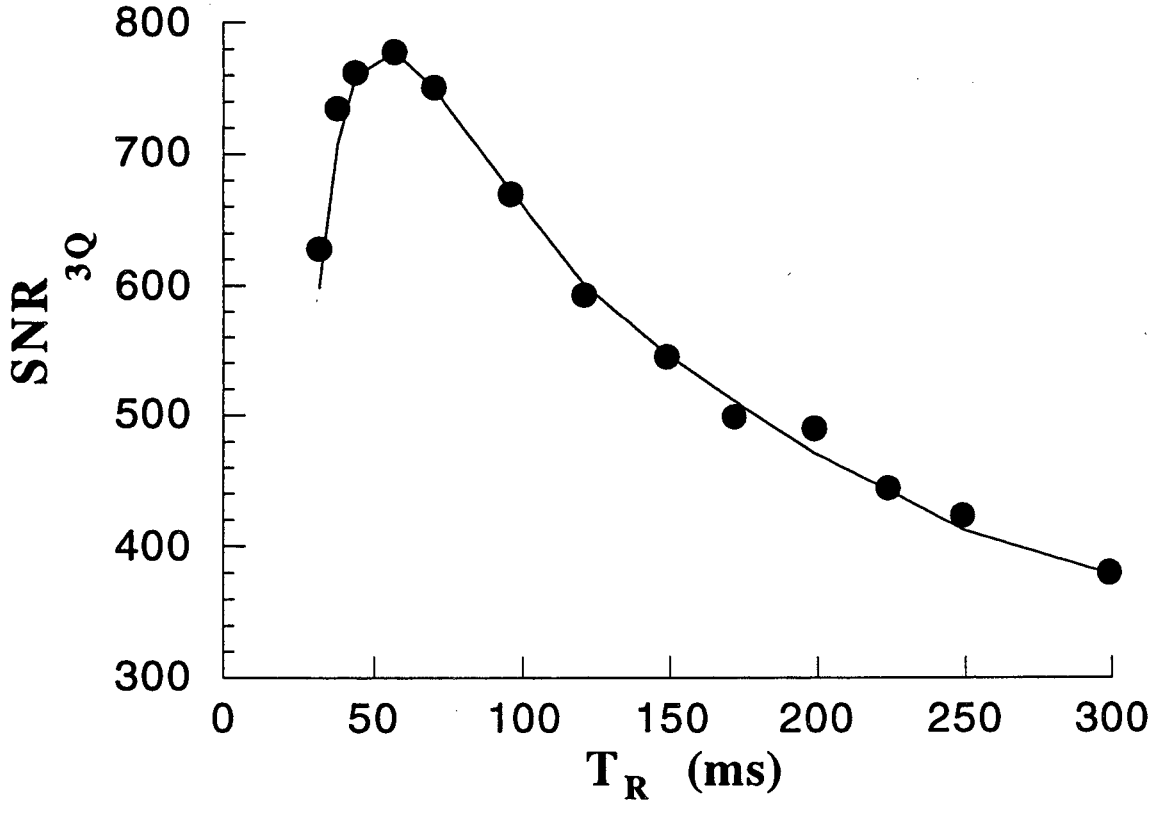

Figure 2

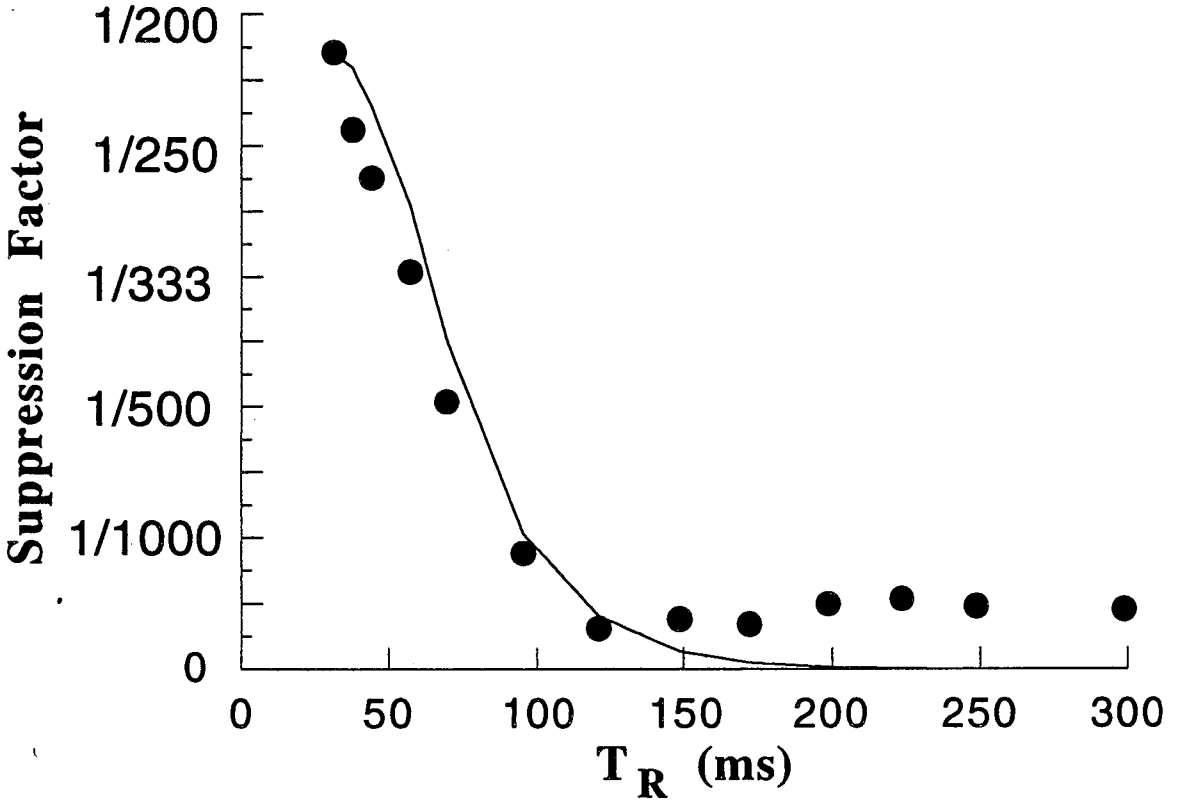
Suppression Factor
1/200
1/250
1/333
1/500
1/1000
0
0
50
100
150
200
250
300
T R (ms)

Figure 3

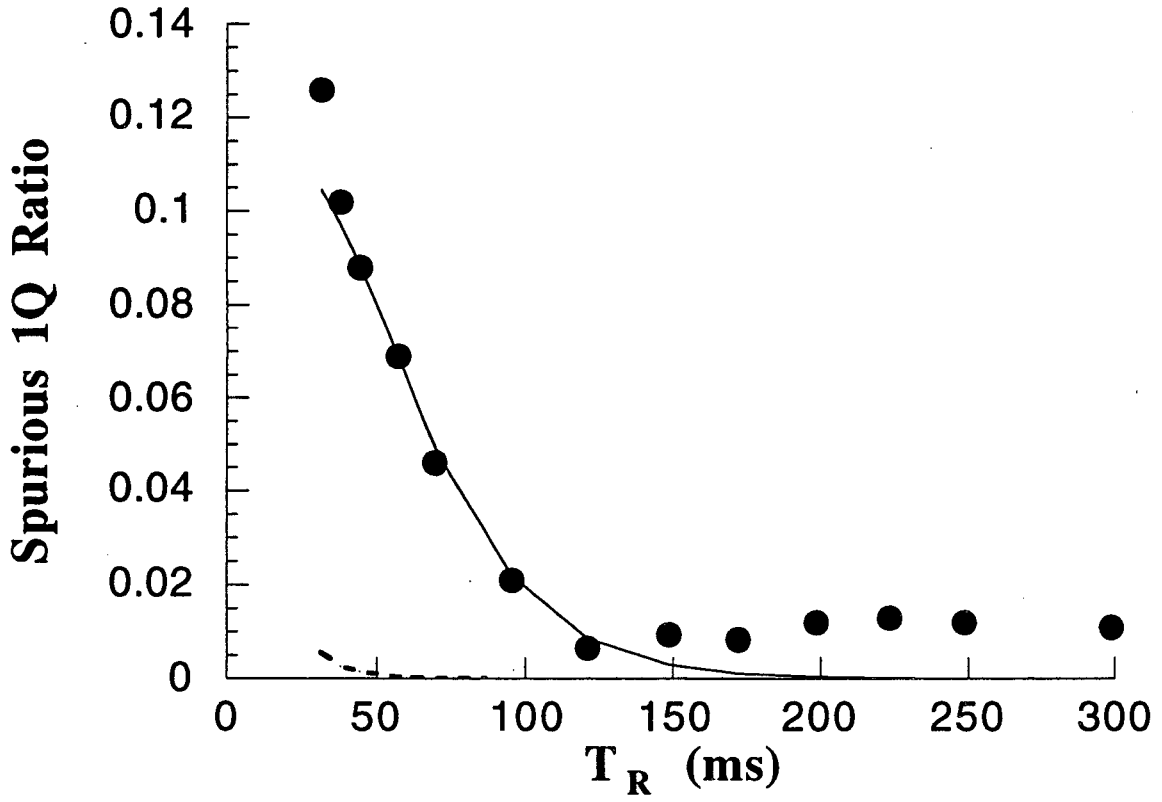
Spurious 1Q Ratio
0.14
0.12
0.1
0.08
0.06
0.04
0.02
0
0
50
100
150
200
250
300
T R (ms)

Figure 4

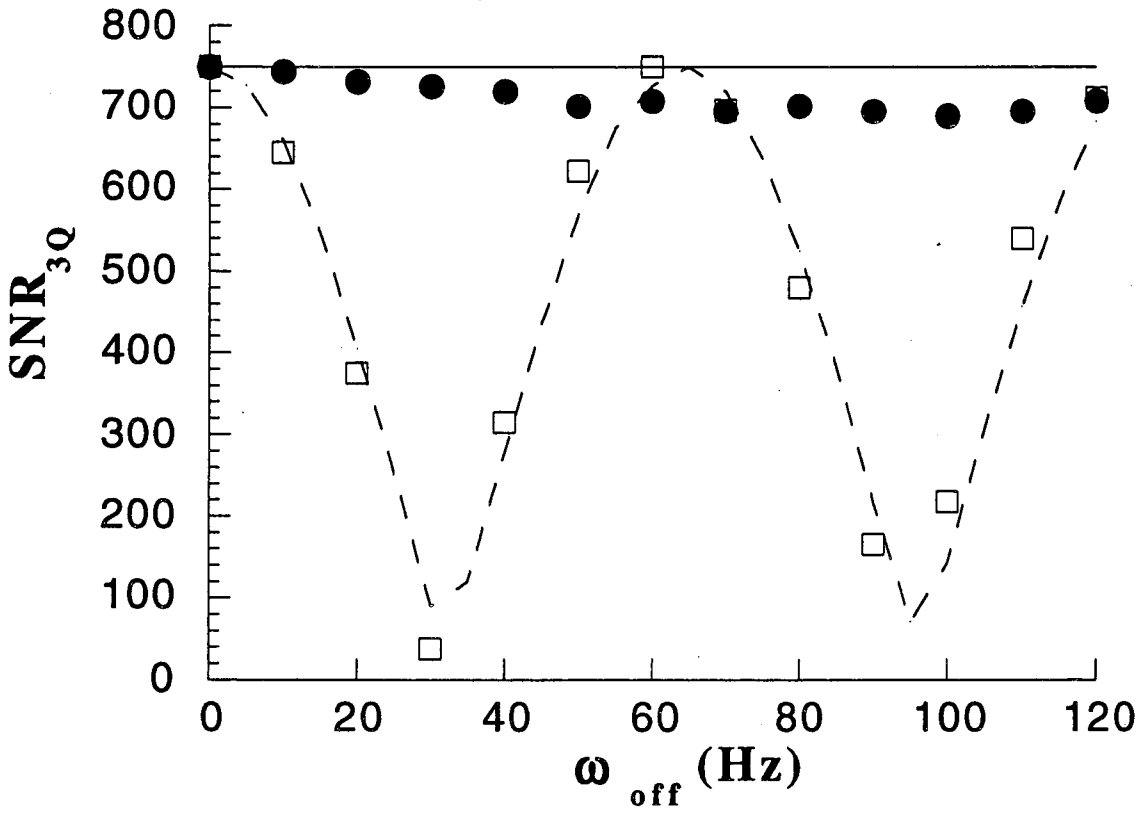
800
700
600
500
400
300
200
100
0
SNR3Q
0
20
40
60
80
100
120
ω off (Hz)

Figure 5

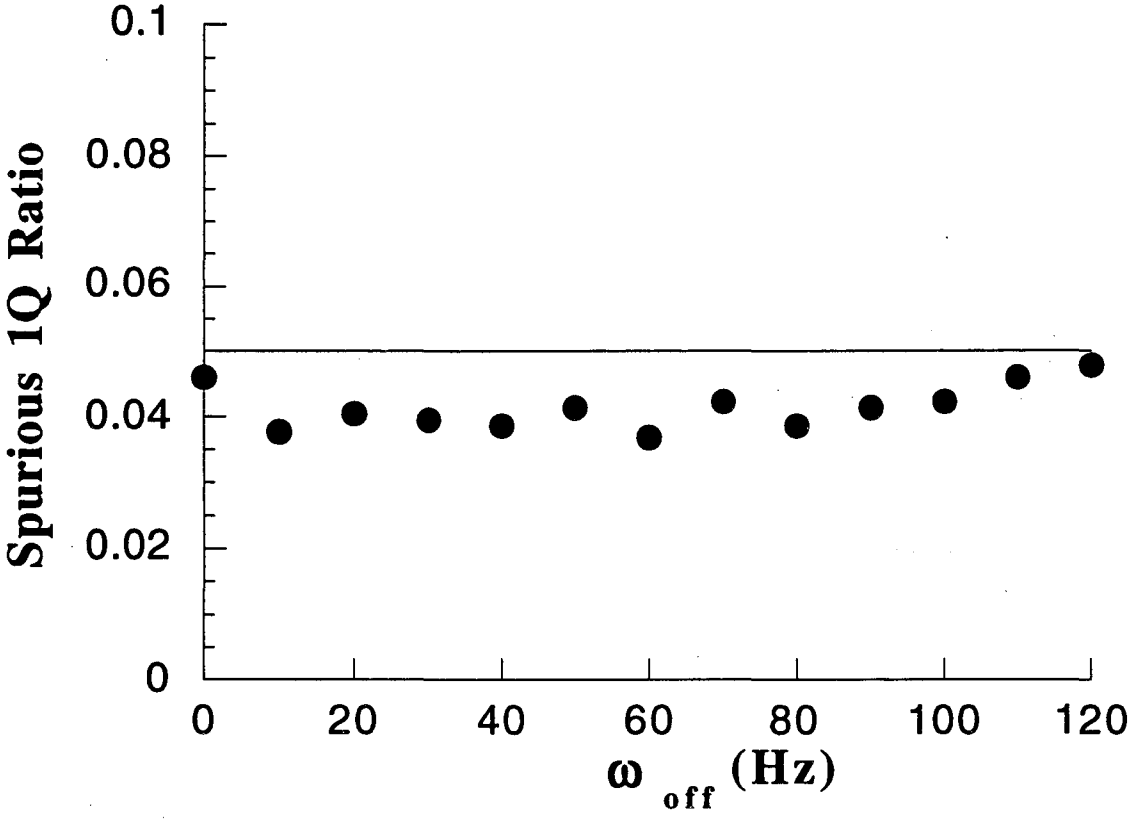
Spurious 1Q Ratio
0.1
0.08
0.06
0.04
0.02
0
0
20
40
60
80
100
120
ω off (Hz)

Figure 6

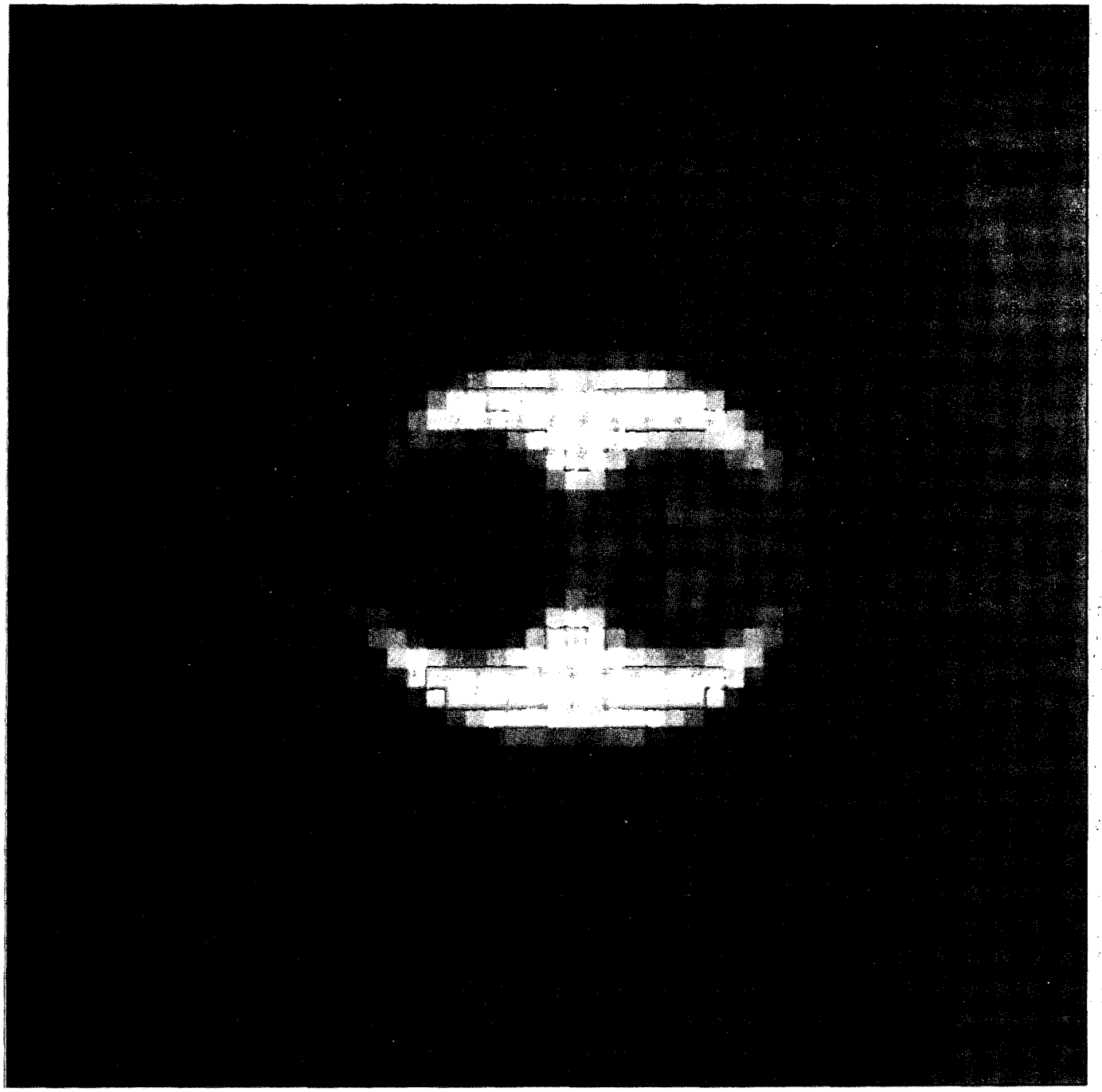

Figure 7

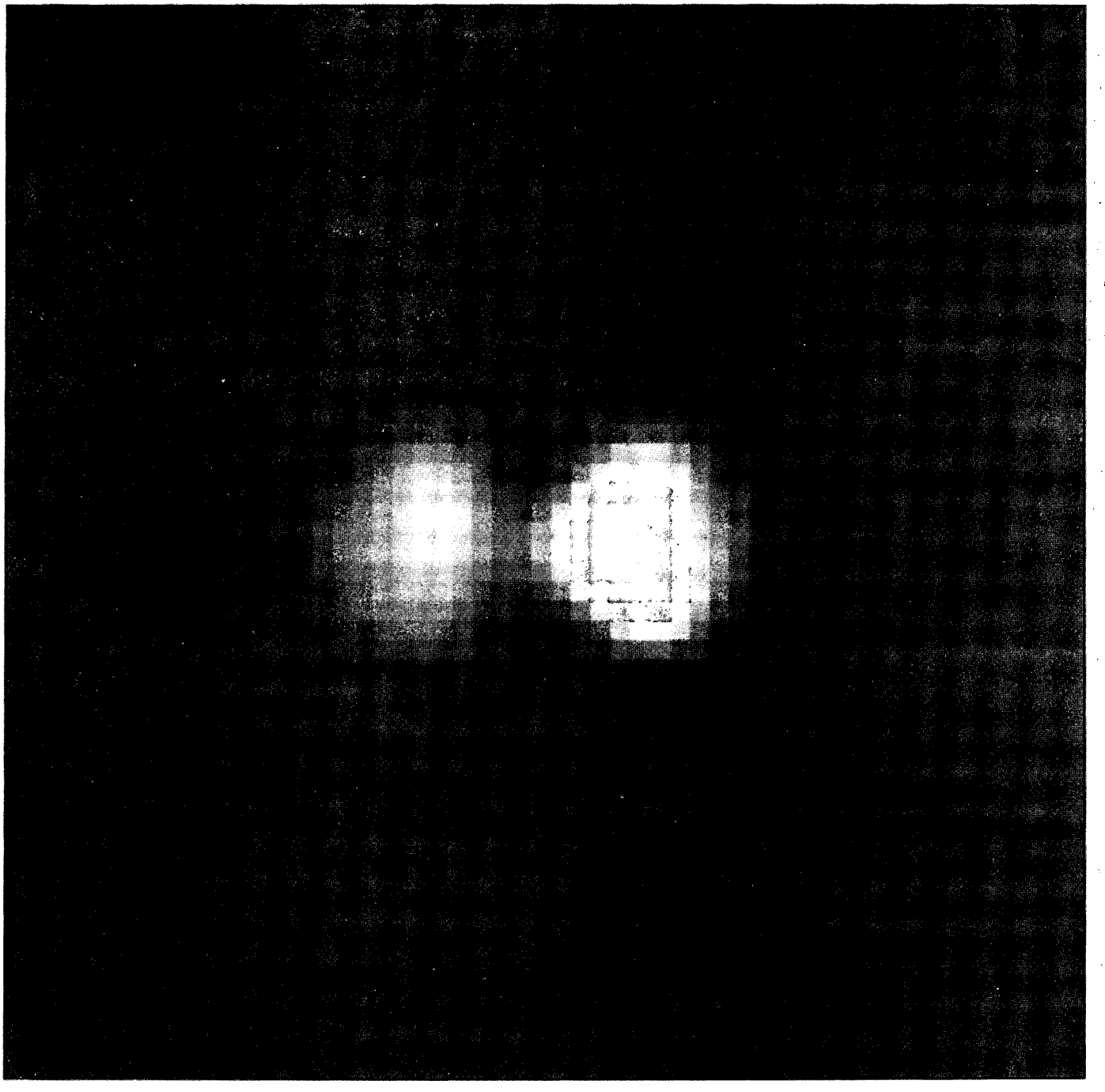

Figure 8

LAWRENCE BERKELEY LABORATORY
UNIVERSITY OF CALIFORNIA
TECHNICAL INFORMATION DEPARTMENT
BERKELEY, CALIFORNIA 94720